Edward Dunham, Peter Collins, Andreas Reinacher and Ulrich Lampater, "SOFIA image motion compensation", Proc. SPIE 7735, 77355X (2010).

http://dx.doi.org/10.1117/12.857731

SOFIA image motion compensation

Edward Dunham[a], Peter Collins[a], Andreas Reinacher[b,c], Ulrich Lampater[b,c]
[a] Lowell Observatory, 1400 W. Mars Hill Road, Flagstaff, AZ 86001, USA;
[b] Deutches SOFIA Institut, Universität Stuttgart, Pfaffenwaldring 31, 70569, Stuttgart, Germany;
[c] SOFIA Airborne Systems Operations Center, NASA Dryden Flight Research Center, Mail Stop DAOF S231, P.O. Box 273, Edwards, CA 93523, USA

ABSTRACT

We describe a laboratory simulation of an image motion compensation system for SOFIA that uses high-speed image acquisition from the science instrument HIPO as the sensing element of the system and a Newport voice-coil actuated fast steering mirror as the correcting actuator. Performance of the system when coupled to the SOFIA secondary mirror is estimated based on the known current performance of the secondary mirror controller. The system is described and the observed performance is presented together with expectations for applicability in flight with SOFIA.

Keywords: SOFIA, Image motion compensation

1. INTRODUCTION

It has been clear for at least a decade that one of the biggest challenges for the SOFIA telescope assembly (TA) will be to meet its pointing stability requirement. The SOFIA Pointing Improvement Team was set up at that time to explore various approaches for improving the telescope's pointing stability[1]. Image motion compensation (IMC) was among the approaches considered at that time. Its application is limited in that a bright natural guide star must be in the vicinity of the astronomical target, but in such cases the compensation is not dependent on the sensitivity of the gyro package to the mode shapes involved.

One IMC application of particular interest to us is supporting precise photometry of extrasolar planet transits. The primary utility of SOFIA in this realm is likely to be observations of the brightest transiting systems where the highest possible signal-to-noise ratio can be achieved and the maximum benefit of SOFIA's stratospheric environment can be realized. Experience with the Kepler testbed[2,3] suggests that image motion will be one of the primary noise sources in the realizing the best photometry. It is this combination of circumstances that motivates us to explore the utility of IMC for SOFIA.

The 26 May 2010 (UT) first-light flight of SOFIA has brought the first actual flight data into consideration and the time has come to pursue IMC in earnest.

1.1 SOFIA telescope vibrational modes

The pointing performance of the SOFIA TA has been extensively modeled by combining its finite element model with a control system model. An example of its expected pointing performance is shown in Figure 7 of reference 1. There is a rather broad spectrum of pointing noise at low frequencies but much of the motion at higher frequencies is expected to be due to a series of resonant modes in the telescope structure. This basic behavior has in fact been observed[4] during the first-light flight. The lowest frequency modes, in the 20-30 Hz range, are due to bending of the Nasmyth tube. The higher frequency modes, ranging from ~45 Hz up to 90-100 Hz, involve structures in the telescope metering structure and mounts for the optical elements.

1.2 Compensation approaches

The lowest frequency disturbances of the TA pointing is due to very low frequency drive forces leaking through the vibration isolation system. These drive the Nasmyth tube bending modes well below their resonant frequencies in a quasi-static manner. A quasi-static flexible body compensation system to correct for this was built in to the TA system long ago, and initial tests suggest that it will be effective. This system uses the fiber optic gyroscopes and

Ground-based and Airborne Instrumentation for Astronomy III, edited by Ian S. McLean, Suzanne K. Ramsay, Hideki Takami, Proc. of SPIE Vol. 7735, 77355X · © 2010 SPIE · CCC code: 0277-786X/10/$18 · doi: 10.1117/12.857731

accelerometers as sensors and the fine drive motors as actuators. A second level of flexible body compensation is also envisioned but not yet implemented. This is the dynamic flexible body compensation, which takes the residual gyro error signals and applies them to the secondary mirror to remove errors at higher frequencies than the fine drive is capable of. However it is only useful for motions sensed by the gyro package and up to the maximum frequency that the secondary mirror can control at small amplitude.

An independent approach that should be useful in the case of a well-defined resonance is the use of active mass dampers mounted to key structural elements. Fortunately it appears that much of the power in the pointing power spectrum is concentrated into relatively narrow regions of the spectrum[4]. This approach should be effective even for the highest frequency modes.

The IMC approach is the last line of defense. It is rather complex and is not universally applicable, but is sensitive to anything that produces unwanted image motion and can compensate up to the limit of the secondary mirror system for small amplitudes. We describe here a prototype IMC system based on a modification of the HIPO science instrument[5] together with the laboratory test system we are using to exercise it. We plan to use the HIPO-based prototype IMC system on early SOFIA flights with HIPO or the co-mounted HIPO and FLITECAM instruments[5] to evaluate the efficacy of IMC for SOFIA to help lay the groundwork for a potential future facility IMC system that would be useful for instruments that benefit from low pointing jitter such as EXES[6] or FLITECAM[7] when it is mounted alone on the TA.

2. TEST SYSTEM OPTICS AND HARDWARE DESCRIPTION

The optics and hardware of the prototype IMC system and its associated laboratory test fixture are described in this section. In overview the prototype IMC system involves a fast CCD mounted in one of the two HIPO dewars with the normal HIPO science CCD mounted in the other dewar. The laboratory system for testing the prototype IMC system mounts to the front of HIPO and produces a focused image at the TA focal plane located inside HIPO. One component of the optical system is a spherical mirror mounted on a voice coil actuator assembly so that image position disturbances can be injected into the system to evaluate the prototype IMC system's ability to reject them. Feedback that would go to the SOFIA secondary mirror assembly in flight instead goes to the correction inputs of the voice coil actuator system.

We note in passing that the laboratory test system is also designed to support precise photometry experiments that will commence later this year. At present this system can illuminate both channels of HIPO simultaneously and we hope to generalize it to include simultaneous illumination of FLITECAM when co-mounted with HIPO. This precise photometry test activity is in the spirit of the Kepler Test Demonstration facility[2,3] and is intended to advance our understanding of the complexities we will face when attempting precise photometric observations in flight.

2.1 Instrument background and modification

The prototype IMC system is a modification of the existing HIPO instrument[5]. The layout of the mechanical and optical parts in HIPO is shown in Figure 1, which is adapted from Figure 1 of reference 5. The only hardware modification needed is to replace one of the standard HIPO CCDs (e2v CCD47-20) with a smaller, faster CCD (e2v CCD67). The CCD67 covers half the linear field as the CCD47 does and has twice the pixel size so the total number of pixels is about 1/16 that of the CCD47. This allows a much faster readout since there are both fewer pixels to read and fewer pixels to skip. In addition the CCD67 is a NIMO part and runs at a much faster parallel clock speed. While the CCD67 can be put in place on either side of HIPO we anticipate that it will normally be on the blue side to allow for Shack-Hartmann testing on the red side. The red side also has a broader operating wavelength range so will generally be preferred for scientific observations. Further information on HIPO may be found in references 5 and 8.

The laboratory test fixture attaches to the front mounting plate of HIPO (item 3 in Figure 1), taking the place of the retaining ring that normally holds the lower part of the FLITECAM periscope in place. This allows the FLITECAM periscope to remain in use for possible future expansion of the system to illuminate FLITECAM along with HIPO. The micrometer that is used to adjust the rotation angle of the lower FLITECAM periscope must be removed when this assembly is mounted. The field lens required to match the pupil position is mounted to the retainer of the HIPO entrance window.

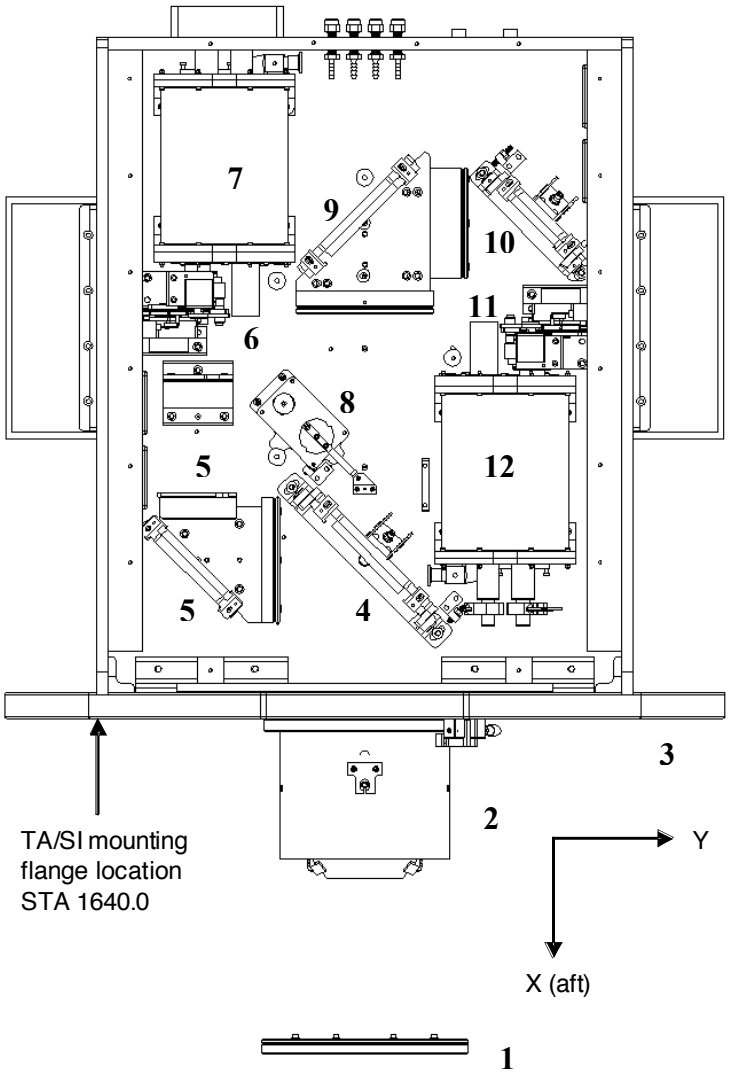

Figure 1. Internal layout of the HIPO instrument.

This figure shows a top view line drawing of HIPO with its cover removed. Light enters the instrument from the bottom of the frame in this view. It first encounters the (optional) gate valve window (1) and the FLITECAM periscope (2) before passing through a window (hidden in this view) mounted in the main mounting flange (3).

The beam is split by a dichroic reflector (4). Shorter wavelengths are reflected toward the blue side collimator (5) that incorporates a fold mirror. The beam traverses the filter wheel and camera lens (6) and enters the blue CCD dewar (7).

The red band transmitted by the dichroic (4) passes the Shack-Hartmann calibration beamsplitter (8) that may be swung in or out of the beam as desired. It then encounters the red collimator with silver-coated fold mirror (9), a second silver-coated fold mirror (10), and finally the red side filter wheel and camera lens assemblies (11) before entering the red CCD's dewar (12).

The HIPO science CCDs are e2v CCD47-20 parts. In the prototype IMC implementation one of these is replaced by an e2v CCD67. Its smaller format allows much higher frame rates to be achieved.

(Adapted from Figure 1 of Reference 5)

2.2 Optical design.

The optical design concept is centered around a small concave spherical mirror that is mounted on a fast tip-tilt stage. This takes the place of the SOFIA secondary mirror and is the stop in the system just as the SOFIA secondary is the stop in the real telescope. In principle the concave spherical mirror could reimage the star plate onto the TA focal plane location, but this would cause the pupil and center of rotation of the mirror to be far too close to the instrument resulting in severe vignetting. A field lens mounted just inside the HIPO optical box causes the spherical fast steering mirror to appear to be the same size and at the same position as the SOFIA secondary mirror. A pellicle beamsplitter is used to prevent the spherical mirror from being operated too far off-axis.

The light source is an incandescent lamp operated at constant current mounted in a 4-inch integrating sphere that in turn is mounted to an 8-inch sphere with a 2-inch exit port diameter. A BG23 filter is in place between the two spheres to create a spectral energy distribution that is relatively close to being solar. The illumination system was procured from Sphere Optics but this company has since been re-integrated with LabSphere. The star plate is mounted at the exit port of the larger integrating sphere. Light from the star plate first reflects off the 4-inch pellicle beamsplitter (CVI Melles

Griot PLB-VIS-xx-40) on its way to the spherical mirror, then transmits through the pellicle as it progresses to the HIPO entrance window (see Figure 2). The integrating sphere, not shown in this figure, is located beneath the star plate.

The fast steering mirror system is an FSM-300-01 from Newport that comes with a 25.4mm diameter flat mirror installed. Newport also has 500 mm radius concave spherical mirrors (10DC500ER.1) with the same diameter and center thickness as the flat that is normally supplied so we bought two of these and two mirror mounts. The spherical mirrors were glued into the mirror mounts with RTV and a spherical mirror/mount combination was installed in place of the standard flat mirror. The field lens is a stock cemented doublet from Ross Optical (L-AOC133/215).

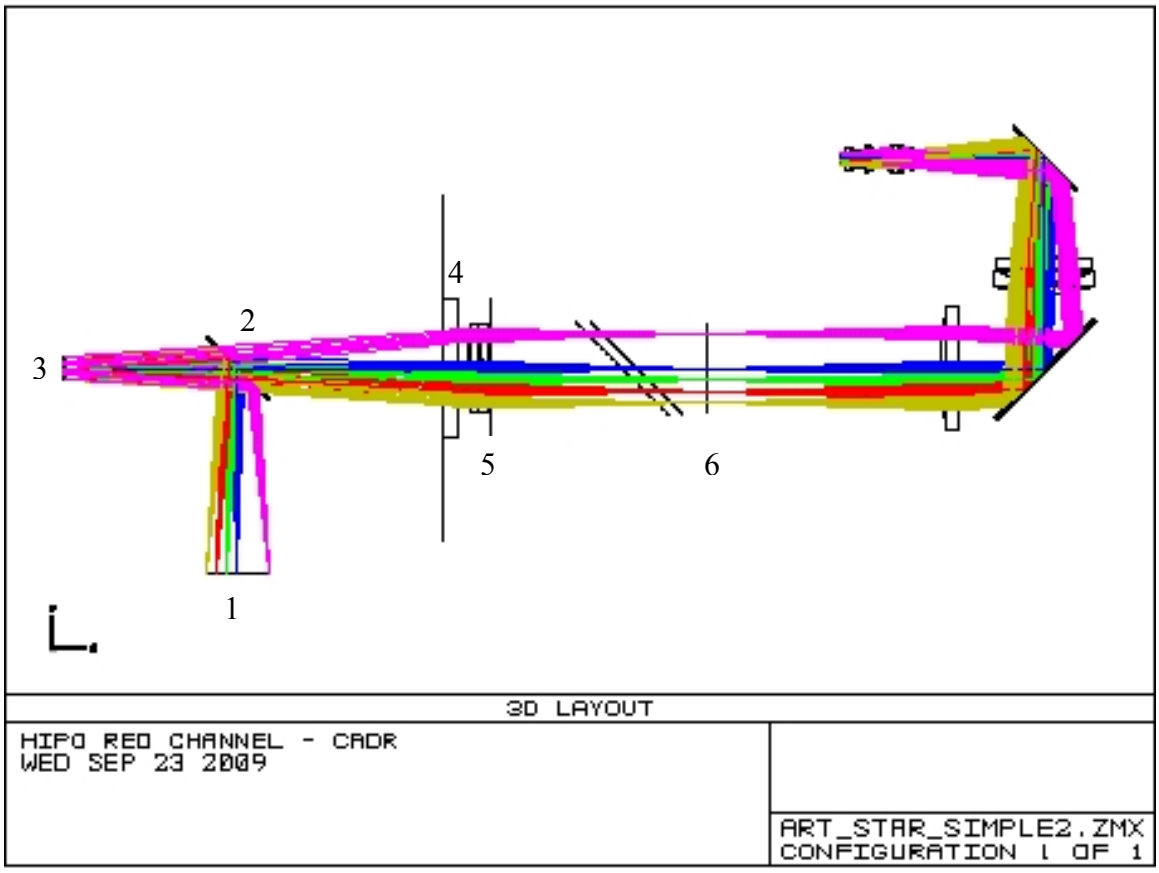

Figure 2. Optical design of the IMC simulation fixture. Light from the star plate (1) reflects off the pellicle beamsplitter (2) to the spherical fast steering mirror (3). The beam progresses through the pellicle beamsplitter (2), through the entrance window (4) and a field lens (5) that causes the fast steering mirror to appear to be at the distance of the SOFIA secondary mirror and also makes the f/ratio match the f/19.6 SOFIA f/ratio. The star plate is imaged at the location of the TA focal plane (6). At this point the optics act the same way they do when the instrument is mounted to the SOFIA TA. The remaining optics shown here are for the HIPO red side but could equally well be for the blue side.

Key properties of the optical system are given in Table 1. A full 256x256 CCD67 frame maps to a 28.0 mm square at the star plate while a full CCD47-20 frame is twice as large. The star plate's clear diameter is 1.75 inch which more than covers the diagonal dimension of the CCD67 but it will cover only part of the CCD47-20 frame. The encircled energy diameters should be compared to the 26 micron CCD67 pixel size which maps to very nearly 2/3 arcsecond when HIPO is mounted to the SOFIA TA. The maximum tilt the steering mirror can execute is ±1.5º for a ±10V input but our DAC can produce only ±5V for a maximum mirror tilt of ±0.75º, corresponding to a ±1.5º tilt of the optical beam and a displacement of the image on the CCD of ±2.12 mm. One count on the DAC corresponds to 1.03 microns of displacement on the CCD.

Table 1. Optical properties of the laboratory test fixture

Paraxial Magnification	0.238 (CCD/Star Plate)			
Tilt/displacement conversion	1.0º mirror tilt = 2.822 mm at CCD			
	Encircled energy diameter (um) Steering mirror centered		Encircled energy diameter (um) Steering mirror tilted 1.0º	
	50% EE	80% EE	50% EE	80% EE
Central field	8.0	15.5	11.0	15.8
24 mm off axis	14.7	23.0	18.6	26.0

2.3 Mechanical design

The mechanical design of the laboratory test fixture is shown in Figures 3 and 4. Figure 3 is a line drawing of the assembly with the left plate removed so the pellicle mount and lower portion of the FLITECAM periscope can be seen. The fixture mounts to the front plate of HIPO by replacing the clamp that holds the lower part of the FLITECAM periscope in place. The field lens is mounted to the entrance window retainer and is on the other side of the main HIPO mounting plate. A possible upgrade to allow the fixture to illuminate FLITECAM also when it is co-mounted will require a new lens located between the lower and upper parts of the FLITECAM periscope. The top of the test fixture will also need to be modified to provide the necessary light path. An image of the completed assembly is shown in Figure 4.

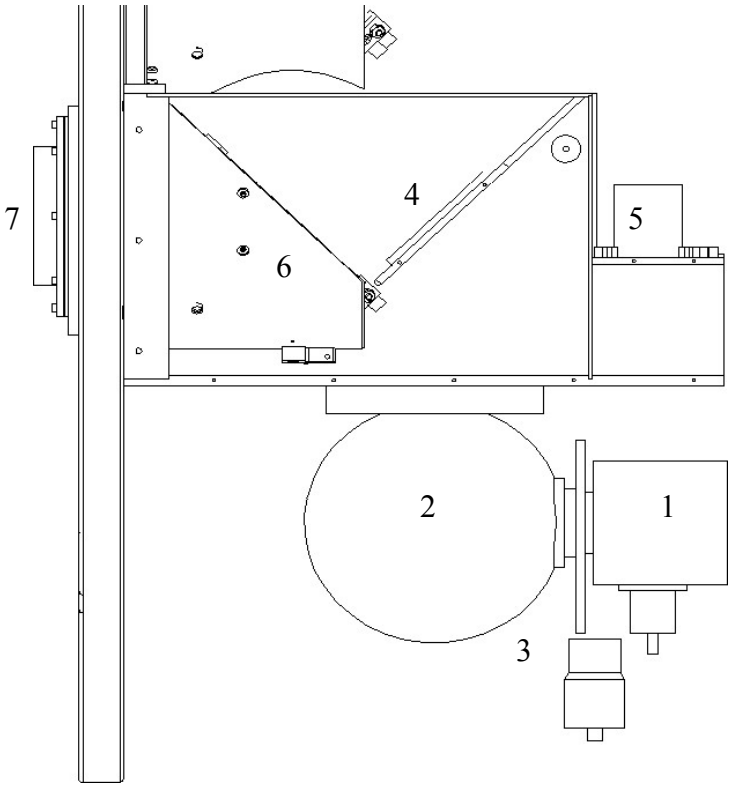

Figure 3. Line drawing of the IMC simulation fixture assembled on the HIPO mounting flange. The left side plate was removed from the solid model in this view so that the internal structure can be seen. The light source is in the small integrating sphere (1) and illuminates the large sphere (2) through the BG23 filter and a variable attenuator (3). The star plate is at the top of the large integrating sphere. From here the light path reflects from the pellicle beamsplitter (4), reflects off the spherical steering mirror (5), passes through the pellicle beamsplitter again and through the lower part of the FLITECAM periscope (6), the HIPO entrance window hidden inside the main mounting flange, and finally through the field lens (7).

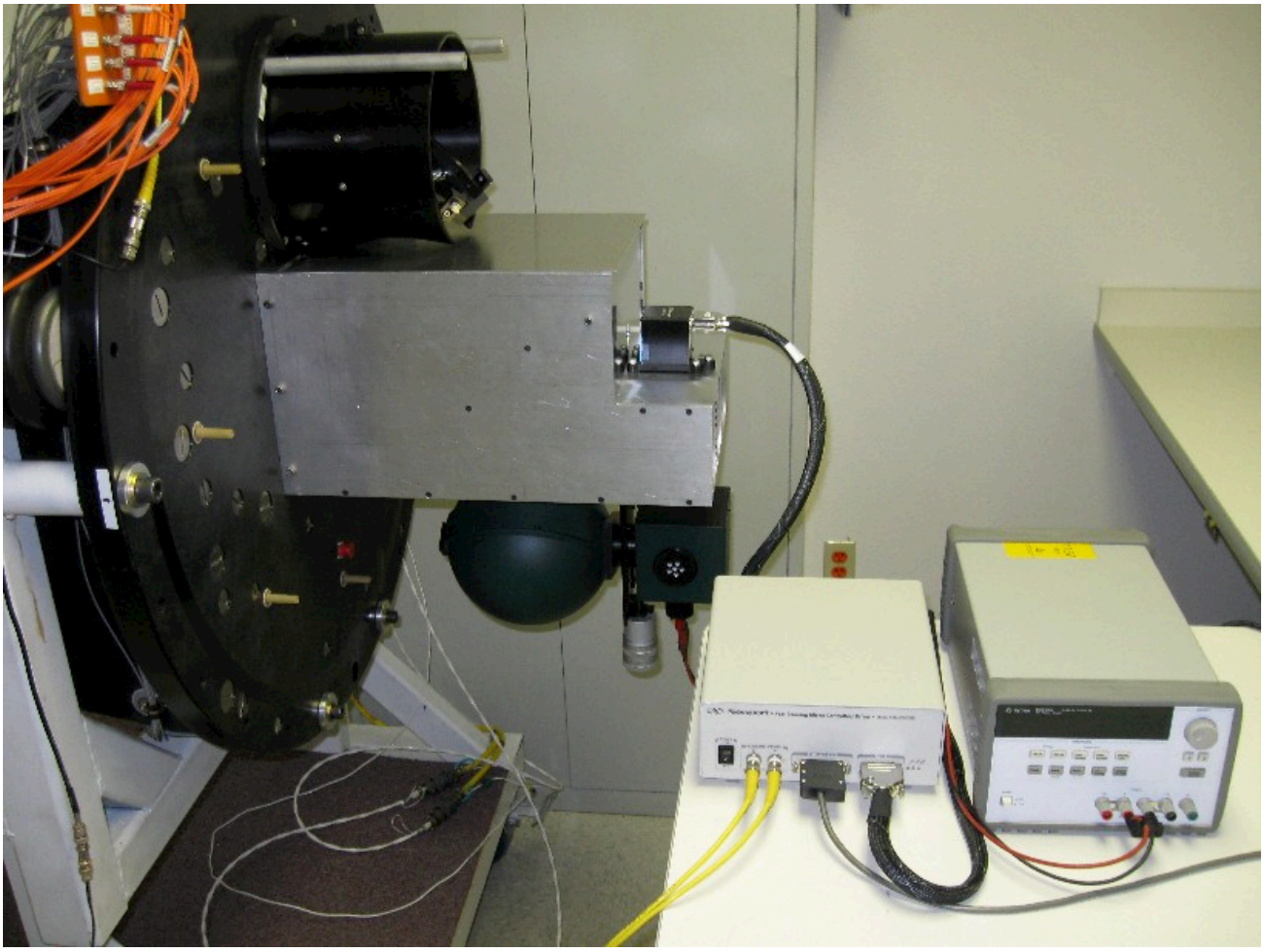

Figure 4. IMC simulation fixture assembled on the HIPO mounting flange. The integrating sphere is attached to the bottom of the fixture and the Newport fast steering mirror head is visible at the right. The fast steering mirror controller is on the bench top (left) next to the power supply for the lamp in the integrating sphere (right).

3. TEST SYSTEM ELECTRONICS AND SOFTWARE DESCRIPTION

3.1 HIPO CCD controller architecture

HIPO uses ARC Gen II CCD controllers[9] for operating the CCDs and for a few ancillary functions. The HIPO hardware design includes the capability of using DACs on the utility board to control the position of the SMA in the SOFIA TA. This capability has now been implemented in software. The main challenges were major changes to the code running in the PCI interface card's DSP to calculate centroids and corrections for the SMA, and dealing with the real-time requirements of a control system as opposed to simple data acquisition.

3.2 System design

The IMC system design is illustrated in Figure 5. For the lab test system described here the SMA is replaced by the Newport Fast Steering Mirror. A simple summing op-amp circuit is needed to sum the control signal from the utility board with a disturbance signal from a signal generator to test the system's ability to correct image motion. The CCD is driven by clock signals from the clock board and biases generated on the video board. Analog processing is done on the video board and all timing functions, including waveform generation, are done on the timing board. The utility board includes the DACs used for generating control signals for the SMA. The PCI interface board normally is used to transfer data to the host computer and send commands to the timing board as well as sending commands to the utility board via

the timing board. In this system the data transfer function has been co-opted for centroid calculation and sending DAC commands to the utility board for SMA position correction.

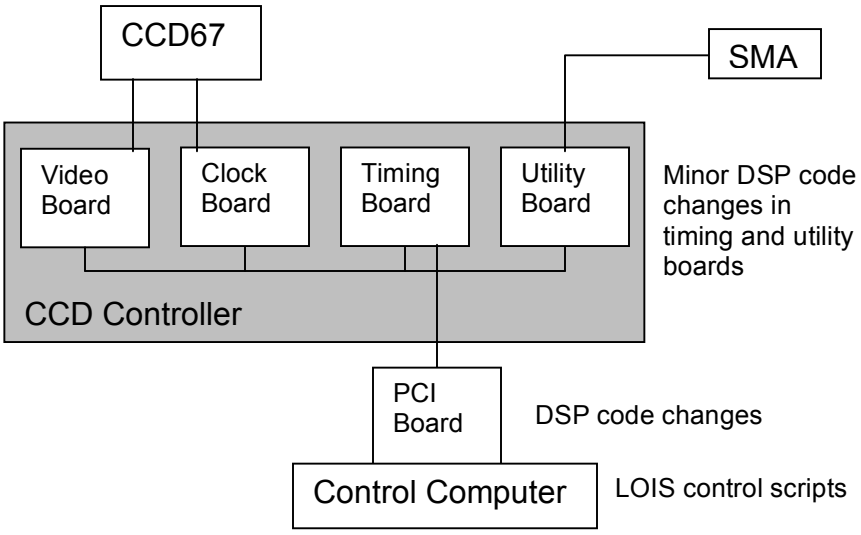

Figure 5. Block diagram of the IMC test system electronics and software with particular emphasis on the software modifications needed to implement the IMC capability. Software changes are primarily in the PCI board's code, secondarily in new LOIS control scripts on the host computer, and minor changes are needed in the timing and utility board code.

3.3 Software Modifications

The HIPO operating software needed modifications in four areas: 1) major modifications to the PCI DSP code; 2) creation of special LOIS scripts on the host computer[8,10] to control the operation of the new PCI code; 3) a minor change to the timing board DSP code; and 4) a minor change to the utility board DSP code. We focus here on the DSP code changes since the LOIS scripts do not represent a change to LOIS and don't affect the performance of the IMC system. In fact LOIS can freely intermix normal data acquisition with IMC operation.

We begin with the simple changes to the timing and utility board DSP code. The only change required in the timing board's code was to inject two additional pixels into the data stream before any real pixels are sent to the PCI card. This allows use of the half-full flag of the FIFO in the PCI board to indicate when 512 pixels of data are available to process. We chose to deal with the buffering effect of the FIFO by limiting ourselves to subframe sizes that are multiples of 512 pixels. Without this modification the real-time requirement of the IMC system could not be met. Except for this modification the timing board uses the HIPO software triggered basic occultation mode[8]. The utility board code was changed by adding a command to write the DACs for controlling both axes of SMA tilt at the same time, and eliminating the "done" response from the command. When the original DAC commands were used there were occasional long delays in the "done" response that had disastrous consequences.

The PCI DSP code begins an IMC run by initializing its variables and initiating the software triggered basic occultation operation. When the FIFO half full flag is set the code reads pixels from the FIFO, fills arrays of flux times X coordinate and flux times Y coordinate, tracks the peak pixel value and location, and accumulates sums of the flux and square of the flux. These calculations occur more quickly than pixel data arrives from the timing board so the code then waits for the next half full flag to repeat this process. When the last buffer of 512 bytes has been processed, additional calculations are done to correct for background and to calculate the intensity-weighted mean centroid. The required SMA tilt corrections are derived by the control law under test and converted to DAC values using a 2x2 matrix multiplication that allows gains, signs, and rotational orientation to be specified.

For test purposes we chose to bin the CCD readout 2x2 with a subframe of 32x32 binned pixels to produce a binned pixel size mapped to the sky of 1.33" and a subframe size of 40" square. The 32x32 subframe contains 1024 pixels or two buffers of half the FIFO length. The seeing-limited image quality at optical wavelengths is expected to be ~5" so the selected pixel size will sample the PSF sufficiently well. The readout time for this subframe depends on its location on the CCD with the fastest readout time being for a subframe located at the corner next to the readout amplifier. For

test purposes we selected this subframe location. The overall timing relationships are detailed in Table 2 for the particular parameters we used for our test work.

Table 2. Timing relationships in the IMC operation

CCD event	Duration (ms)	Timing board event	Duration (ms)	PCI board event	Duration (ms)
Frame transfer	0.33	Frame Transfer	0.33	Wait for first half-full flag	1.00
Integrate in image area	2.34	Read first 512 pixels	0.67		
		Read second 512 pixels	0.67	First half-full flag set Do pixel-level calculations	0.60
				Wait for second half-full flag	0.07
		Go to EXPOSE function for 1 ms exposure time. Process DAC command when it arrives.	1.00	Second half full flag set Do pixel-level calculations	0.60
				Complete centroid calculation Generate and send DAC command	0.12
				Wait for first half-full flag	0.28

The PCI DSP code provides a number of checks to guard against possible bad IMC corrections. Pixels around the edge of the image are cropped to avoid problems related to the two additional injected pixels described earlier. A signal level check is done and corrections are not issued for images that are too faint. The centroid calculation is done in a box of pixels that is a subset of the cropped image and centered on the peak pixel. If the centroid box is too close to the image edge no correction is calculated or issued. Background tracking is done using the pixels in the cropped subframe that are outside of the centroid box. A rolling average of background for 8 frames is maintained. This rolling average is updated for all frames that pass a variance test. Those with too high variance are not accumulated in the rolling average in order to reject cosmic rays.

In addition to the basic IMC operation described above the code maintains a wide range of diagnostic data that can be read out of the DSP memory with appropriate LOIS TCL scripts after the run is complete. These diagnostics include information on times at which several check points are reached and the observed centroids together with the calculated corrections.

To date we have only attempted a simple proportional correction scheme whereby the previous DAC setting is changed by the value derived from the observed offset of the image centroid from its desired target location. The gain in this proportionality (in units of DAC counts per pixel of offset) is a free parameter that can be changed to optimize performance.

4. TEST RESULTS

The key parameters of an IMC system are the frame rate and latency between the middle of the exposure and generation of the correction signal. From Table 2 the frame time is 2.67 ms corresponding to a frame rate of about 375 Hz. The latency is half of the CCD integration time plus all the times down to generation of the DAC command for a total latency of 3.56 ms. This corresponds to a 90° phase lag at a frequency of 70 Hz. The fast steering mirror is much faster than this with a phase lag of only 5° at 70 Hz and 90° at 700 Hz. The expected frequency for 90° phase lag of the combined IMC sensing and feedback system is about 60 Hz.

Not surprisingly the simple proportional control algorithm tested to date provides a lower bandwidth than might be expected. Figure 6 shows the performance of the system as correction achieved as a function of frequency with a sinusoidal disturbance applied (left panel) and step response (right panel) for three different proportional gain settings. The left panel shows that the magnitude of the sinusoidal image disturbance is reduced by 50% at 20 Hz with better corrections achieved at lower frequencies. The right panel shows overshoot and ringing that increases with gain. The gain used for the sinusoidal correction cases result in unstable behavior when a step function is applied. Implementation of a full PID controller will be pursued and is expected to improve the performance of this system substantially.

The Newport fast steering mirror is much faster than the SOFIA SMA, which currently reaches 90° phase lag at 30 Hz. When coupled with the SOFIA SMA the maximum lag of the HIPO IMC system will increase resulting in an expected 90° phase lag at about 20 Hz.

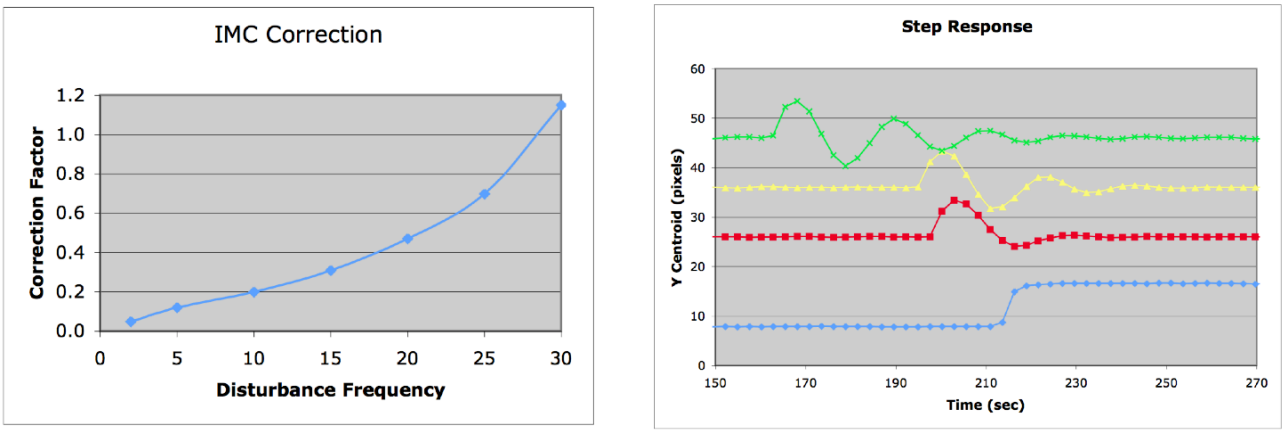

Figure 6. Measured performance of the IMC system using the proportional control algorithm. The left panel shows the ratio of the observed corrected rms motion to the rms of a sinusoidal disturbance as a function of disturbance frequency. These were done with gain settings of 20-21 DAC ADUs per pixel. Higher gains were unstable at the higher disturbing frequencies. The right panel shows the step response of the system. The step input is shown in the bottom trace and the corrected step responses for gain settings of 10, 15, and 17 DAC ADUs per pixel are shown from bottom to top. Higher gains were unstable.

5. CONCLUSIONS

The HIPO IMC concept described here achieves useful correction up to 20 Hz with a simple proportional control algorithm and should be capable of achieving reasonable correction at 40-50 Hz with a full PID controller. Faster instrument-specific systems could be produced using different hardware approaches. As currently configured the SMA controller reaches a 90° phase lag at about 30 Hz and when coupled with the HIPO IMC system with improved control algorithm would likely have a 90° phase lag at about 20 Hz. This suggests two possible implementations for SOFIA applications: 1) instrument-specific IMC systems with small actuators that can operate at high frequencies and 2) facility-level IMC systems limited to lower frequencies by the much larger secondary mirror.

The first flight data[4] indicate that most of the power in the pointing error is at frequencies < 10 Hz with most of the remaining power being in specific modes with frequencies ranging from ~45-100 Hz. The Nasmyth tube bending modes in the 20-30 Hz range had low amplitude during this flight, presumably due to calm flight conditions. The disturbances below 10 Hz should be visible to the gyros since they primarily represent rigid body motions of the TA and should be correctable either by tuning the fine drive controller or by using the dynamic FBC approach. The higher frequency modes are faster than the expected small-signal bandwidth of the present SMA and will have to be corrected either with mass dampers, a facility IMC system using a new SMA with higher bandwidth, or fast instrument-specific IMC systems. The IMC approach may have utility in correcting any lower frequency disturbances that turn out to be difficult to correct by other means, but the other approaches should be explored first.

REFERENCES

[1] Süss, M., K. Wandner, H.J. Kärcher, P. Eisenträger, and U. Schönhoff, "Airborne Pointing and Pointing Improvement Strategy for SOFIA", Proc. SPIE 4857, 372-381 (2003).

[2] Koch, D.G., W. Borucki, E. Dunham, J. Jenkins, L. Webster, and F. Witteborn, "CCD photometry tests for a mission to detect Earth-size planets in the extended solar neighborhood", Proc. SPIE 4013, 508-519 (2000).

[3] Jenkins, J.M., F. Witteborn, D.G. Koch, E. Dunham, W.J. Borucki, T.F. Updike, M.A. Skinner, and S.P. Jordan, "Processing CCD images to detect transits of Earth-sized planets: Maximizing sensitivity while achieving reasonable downlink requirements", Proc. SPIE 4013, 520-531 (2000).
[4] Herter, T., private communication, (2010).
[5] Dunham, E.W., J.L. Elliot, T.A. Bida, and B.W. Taylor, "HIPO – A High-speed Imaging Photometer for Occultations", Proc. SPIE 5492, 592-603 (2004).
[6] Richter, M.J., et al., "High-resolution mid-infrared spectroscopy with EXES and SOFIA", Proc. SPIE 4857, 37-46 (2003).
[7] McLean, I.S., et al., Proc. SPIE 6269, 168 (2006).
[8] Dunham, E.W., J.L. Elliot, T.A. Bida, P.L. Collins, B.W. Taylor, and S. Zoonematkermani, "HIPO Data Products", Proc. SPIE 7014, 70144Z-1-70144Z-10 (2008).
[9] Leach, R.W., F.L. Beale, and J.E. Eriksen, "New-generation CCD controller requirements and an example: The San Diego State University generation II controller", Proc. SPIE 3355, 512-519 (1998).
[10] Taylor, B.W., E.W. Dunham, and J.L. Elliot, "Performance of the Lowell Observatory Instrumentation System", Proc. SPIE 5496, 446-454, (2004).